

## Synthesis and Solid-State Study of Supramolecular Host–Guest Assemblies: Bis[6-*O*,6-*O'*-(1,2:3,4-diisopropylidene- $\alpha$ -D-galactopyranosyl)thiophosphoryl] Dichalcogenides

Marek J. Potrzebowski,<sup>\*,†</sup> Wojciech M. Potrzebowski,<sup>‡</sup> Agata Jeziorna,<sup>†</sup> Włodzimierz Ciesielski,<sup>†</sup> Jarosław Gajda,<sup>†</sup> Grzegorz D. Bujacz,<sup>⊥</sup> Maksymilian Chruszcz,<sup>§</sup> and Wlodek Minor<sup>§</sup>

Polish Academy of Sciences, Centre of Molecular and Macromolecular Studies, Sienkiewicza 112, 90-363 Łódź, Poland, Department of Physics, Technical University of Łódź, Wólczajska 215, 93-005 Łódź, Poland, Department of Molecular Physiology and Biological Physics, University of Virginia, 1340 Jefferson Park Avenue, Charlottesville, Virginia 22908-0736, and Institute of Technical Biochemistry, Technical University of Łódź, Stefanowskiego 4/10, 90-924 Łódź, Poland

marekpot@cbmm.lodz.pl

Received November 20, 2007

A complementary approach for studying structural details of complex solid materials formed by symmetrical and unsymmetrical dichalcogenides, which employs both X-ray diffraction (XRD) and solid-state NMR (SS NMR), is presented. The new diagnostic technique allows reversible crystallographic space group change and very subtle distortion of host geometry to be followed during guest migration in the crystal lattice. Bis[6-*O*,6-*O'*-(1,2:3,4-diisopropylidene- $\alpha$ -D-galactopyranosyl)]thiophosphoryl selenenyl sulfide, a representative of wheel-and-axle host (WAAH) molecules, can be synthesized in the solid state by grinding and gentle heating of disulfide **1** and diselenide **2**. Full characterization of disulfide **1** in the solid phase has been reported (*J. Org. Chem.* 1995, 60, 2549). In the current work, the synthesis and both XRD and SS NMR studies of the isostructural diselenide substrate **2** are presented. A <sup>31</sup>P cross polarization magic angle spinning experiment is employed to follow the progress of synthesis of selenenyl sulfide **3** in the solid state. It is concluded that selenenyl sulfide exists in equilibrium with disulfide and diselenide in a 1:1:1 ratio in both the liquid and the powdered solid. A mixture of isostructural dichalcogenides crystallized from different solvents form three-component host–guest inclusion complexes with columnar architecture. In the host–guest complex of diselenide **2** with toluene (space group *C*<sub>2</sub>), columns of host molecules are in parallel orientations along all the axes, whereas in the structures of diselenide **2** with propan-2-ol and propan-1-ol (space group *P*3<sub>2</sub>), the columns of host molecules lay along the 3-fold symmetry axis. Thermal processes effecting structural changes in the host lattice and the kinetics of reversible guest molecule diffusion were investigated using SS NMR spectroscopy. Finally, the Se/S scrambling phenomenon and limitations in the X-ray structure refinement of organic compounds containing selenium and sulfur in chains are discussed.

### Introduction

Wheel-and-axle host (WAAH) molecules have received a great deal of attention due to their prospective applications in the design of new soft supramolecular materials.<sup>1</sup> This class of compounds is attractive because in the presence of neutral molecules of another component (guest), such species can form porous structures with intriguing and sometimes unpredictable architecture. Unlike most organic molecules that crystallize as

single-component crystals, WAAH species are unable to pack properly because of their shape and thus crystallize only with the inclusion of a guest. The common feature of WAAH molecules is the presence of two bulky fragments connected by a bridging spacer. The spacers may vary in shape, rigidity, or flexibility. Bridges usually consist of directly bonded acetylenic units or units separated by an aromatic group (Scheme 1). The WAAH molecules can also be classified as a group of molecular machines, as recently described by Garcia-Garibay et al.<sup>2</sup>

The strong tendency to form inclusion complexes by bis[6-*O*,6-*O'*-(1,2:3,4-diisopropylidene- $\alpha$ -D-galactopyranosyl)thiophosphoryl] disulfide **1** (Scheme 2) as a WAAH molecule has

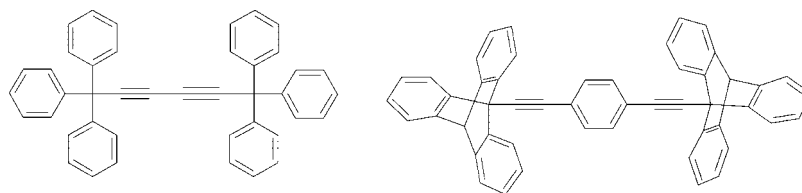
<sup>†</sup> Polish Academy of Sciences.

<sup>‡</sup> Department of Physics, Technical University of Łódź.

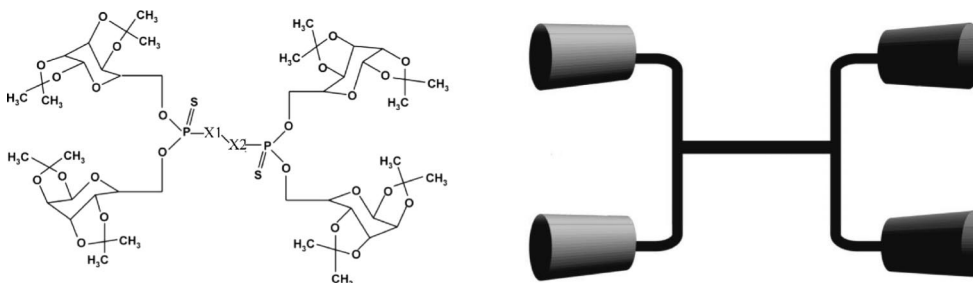
<sup>§</sup> University of Virginia.

<sup>⊥</sup> Institute of Technical Biochemistry, Technical University of Łódź.

## SCHEME 1



## SCHEME 2



**1:** X1=X2=S; **2:** X1= X2=Se; **3:** X1=S, X2=Se

been shown in a number of papers published elsewhere.<sup>3</sup> Compared to the classical representative of WAAH compounds, **1** can be called a “four-wheeled system”. Guest molecules might be incorporated into the space between the “front wheels” (or “rear wheels” or both) of **1**. Herein we report the synthesis and structural studies of WAAH compounds very similar to **1** with a diselenide spacer (compound **2**) and a selenenyl-sulfide spacer (compound **3**) between phosphorus atoms.

It is well-known that upon guest removal, the host molecules may retain their structure. A change or collapse depends on the stability of the host framework.<sup>4</sup> In this work, we reveal that high-resolution solid-state NMR spectroscopy is an excellent diagnostic technique that allows very subtle changes of host geometry to be followed during guest migration in the crystal lattice. As a result of the presence of phosphorus nuclei (<sup>31</sup>P) in the bridging spacer, a cross-polarization magic angle spinning (CP/MAS) experiment was found to be the method of choice for the study of **1**. By including selenium-containing molecules in the model, we have an additional structural probe that allows extension of the NMR studies with <sup>77</sup>Se CP/MAS experiments.

Selenium–sulfur bonds play an important role in inorganic, organic, and biological systems. Selenium-containing proteins often possess a selenosulfide linkage, which is typically formed through redox chemistry or nucleophilic attack at the sulfur or selenium end. As reported in a number of papers, such species

are postulated as intermediates in the catalytic cycle of glutathione peroxidase (GPx) and its synthetic model compounds.<sup>5</sup>

The synthesis and characterization of selenenyl sulfides (R-S-Se-R') is still a challenge for organic chemistry. It is known that selenenyl sulfides are unstable and undergo disproportionation reactions to give the corresponding disulfide (R-S-S-R) and diselenides (R'-Se-Se-R').<sup>6</sup> However, as reported by Kice and Lee, usually disproportionation is slow compared to the relatively rapid reaction between substrates, e.g., selenenyl bromide and thiols.<sup>7</sup>

A preliminary study of three-component crystals (TCC) consisting of **1**, **2**, and **3** have been published.<sup>8</sup> In this paper, new aspects related to solid-state synthesis in the NMR rotor and methodology for investigation of reversible guest exchange employing solid-state NMR are presented. Moreover, atom scrambling phenomena observed in the refinement of X-ray structures of chemically similar compounds is discussed.

## Results and Discussion

**1. Synthesis and Solid-State NMR Study of Bis[6-O,6-O'-(1,2:3,4-Diisopropylidene- $\alpha$ -D-galactopyranosyl)thiophosphoryl] Dichalcogenides.** In our recent paper, we have shown that bis[6-O,6-O'-(1,2:3,4-diisopropylidene- $\alpha$ -D-galactopyranosyl)thiophosphoryl] selenenyl-sulfide **3** can be synthesized in the reaction of appropriate selenyl bromide and triethylamine dithiophosphoryl salt.<sup>8</sup> In this reaction, compound **3** is obtained with ca. 30% yield. The other products are diselenide **2** and disulfide **1**. The ratio of the three products is 1:1:1, and this proportion is preserved both in the liquid phase and for powdered sample in the solid state. In this paper, we report a

(1) Soldatov, D. V. *J. Chem. Crystallogr.* **2006**, *36*, 747–768, and references therein.

(2) Khuong, T. A. V.; Nunez, J. E.; Godinez, C. E.; Garcia-Garibay, M. A. *Acc. Chem. Res.* **2006**, *39*, 413–422, and references therein.

(3) (a) Potrzebowski, M. J.; Helinski, J.; Olejniczak, S.; Ciesielski, W. *J. Phys. Org. Chem.* **2006**, *19*, 53–60. (b) Potrzebowski, M. J.; Kazmierski, S. *Top. Curr. Chem.* **2005**, *246*, 91–140. (c) Potrzebowski, M. J.; Grossmann, G.; Ganicz, K.; Olejniczak, S.; Ciesielski, W.; Kozioł, A. E.; Wawrzycka, I.; Bujacz, G.; Haeblerl, U.; Schmitt, H. *Chem. Eur. J.* **2002**, *8*, 2691–2699. (d) Potrzebowski, M. J.; Ganicz, K.; Ciesielski, W.; Skowronka, A.; Wiczorek, M. W.; Blaszczyk, J.; Majzner, W. *J. Chem. Soc., Perkin Trans. 2* **1999**, *10*, 2163–2170. (e) Potrzebowski, M. J.; Blaszczyk, J.; Wiczorek, M. W. *J. Org. Chem.* **1995**, *60*, 2549–2562.

(4) (a) Kitagawa, S.; Kondo, M. *Bull. Chem. Soc. Jpn.* **1998**, *71*, 1739–1753. (b) Soldatov, D. V.; Ripmeester, J. A. In *Nanoporous Materials IV: Organic Zeolites*; Sayari, A. Ed.; Elsevier: Amsterdam, 2005; pp 37–54.

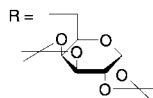
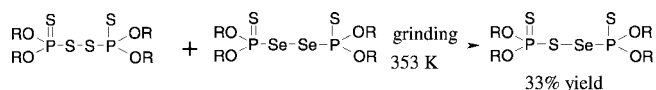
(5) (a) Back, T. G.; Dyck, B. P. *J. Am. Chem. Soc.* **1997**, *119*, 2079–2083. (b) Mugesh, G.; Singh, H. B. *Chem. Soc. Rev.* **2000**, *29*, 347–357, and references therein.

(6) (a) Bergson, G.; Nordstroem, G. *Ark. Kemi* **1961**, *17*, 569–577. (b) Potapov, V. A.; Amosova, S. V.; Petrov, P. A.; Romanenko, L. S.; Keiko, V. V. *Sulfur Lett.* **1992**, *15*, 121. (c) Ahrika, A.; Auger, J.; Paris, J. *New J. Chem.* **1999**, *23*, 679–681.

(7) Kice; J. L.; Lee, T. W. S. *J. Am. Chem. Soc.* **1978**, *100*, 5094–5102.

(8) Potrzebowski, M. J.; Helinski, J.; Ciesielski, W. *Chem. Commun.* **2002**, 1582–1583.

## SCHEME 3



full description of the method of synthesis, a new approach for the preparation of **3**, which is based on solid-state synthesis methodology, and an explanation of the relatively low yield of **3**. The appropriate substrates necessary for synthesis of **3** were obtained employing the dithiaphospholane approach.<sup>9</sup>

In the wet chemistry approach, sample **3** can be also obtained in a reaction of the appropriate ammonium salts or in a reaction of **1** and **2**. Progress of the reaction can be monitored by liquid-state <sup>31</sup>P NMR. After reacting overnight in an NMR tube, we have an equimolar mixture of three components. It has to be stressed that such a mixture can be obtained in the solid state. By handle grinding of mixture **1** and **2**, only a small increase in the amount of **3** was observed. Much better results were obtained when a sample was gently heated to 353 K and ground (Scheme 3). A thermal treatment of samples is a commonly used approach in solid-state synthesis.<sup>10</sup> Employing such a procedure resulted in **3** with a 33% yield, exactly the same as in the liquid state. Details describing the formation of **3** in the solid state are discussed in section 2.

Figure 1 shows the solid-state NMR spectra of the inclusion complex of **2A** with toluene as a guest in the crystal lattice. The presence of broad distorted signals (Figure 1a) suggests that the asymmetric unit contains more than one molecule of **2**. However, care has to be taken in the interpretation of data for systems possessing two chemically equivalent nuclear spins with 100% natural abundance. Wu and Wasylishen have revealed that MAS NMR spectra arising from a pair where nuclear spins are not related by a center of inversion are sensitive to sample spinning frequency.<sup>11</sup>

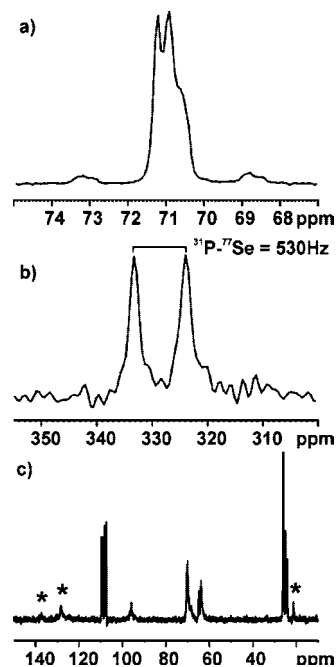
Figure 2 displays the <sup>31</sup>P CP/MAS spectra for **2A** recorded with a spinning rate in the range of 2–8 kHz. It is apparent that the <sup>31</sup>P NMR line shape is strongly dependent on sample spinning. A change of line shape is related to the *J*-coupling effect between chemically equivalent spins and is enhanced by differences in the orientations of their respective chemical shift tensors and by the strength of direct homonuclear coupling. Thus, we can assume that only half of the molecule of **2** is an asymmetric unit. Such an assumption is consistent with the <sup>77</sup>Se CP/MAS spectrum shown in Figure 1b. The two lines observed in the isotropic region are due to the presence of only one type of crystallographically and magnetically nonequivalent selenium atoms and <sup>31</sup>P–<sup>77</sup>Se *J*-coupling. The presence of toluene in the crystal lattice was confirmed by a <sup>13</sup>C CP/MAS experiment (Figure 1c). The signals coming from the guest molecule are labeled by asterisks.

Figure 3a shows the <sup>31</sup>P CP/MAS spectrum of the powdered sample (PS) of TCC with occluded toluene in the crystal lattice.

(9) (a) Stec, W. J.; Grajkowski, A.; Karwowski, B.; Kobylanska, A.; Koziolkiewicz, M.; Misiura, K.; Okruszek, A.; Wilk, A.; Guga, P.; Boczkowska, M. *J. Am. Chem. Soc.* **1995**, *117*, 12019–12029. (b) Baraniak, J.; Korczynski, D.; Stec, W. J. *J. Org. Chem.* **1999**, *64*, 4533–4536. (c) Baraniak, J.; Kaczmarek, R.; Stec, W. J. *Tetrahedron Lett.* **2000**, *41*, 9139–9142.

(10) Tanaka, K.; Toda, F. *Chem. Rev.* **2000**, *100*, 1025–1074, and references therein.

(11) (a) Wu, G.; Wasylishen, R. E. *J. Chem. Phys.* **1993**, *98*, 6138–6149. (b) Wu, G.; Wasylishen, R. E. *Inorg. Chem.* **1996**, *35*, 3113–3116.



**FIGURE 1.** CP/MAS spectra of host–guest complex **2A** with toluene in the crystal lattice recorded with a spinning rate of 8 kHz. (a) Isotropic part of the 121.49 MHz <sup>31</sup>P spectrum. (b) Isotropic part of the 57.24 MHz <sup>77</sup>Se spectrum. (c) 75.47 MHz <sup>13</sup>C CP/MAS spectrum. Signals representing the toluene guest molecule are labeled by asterisks.

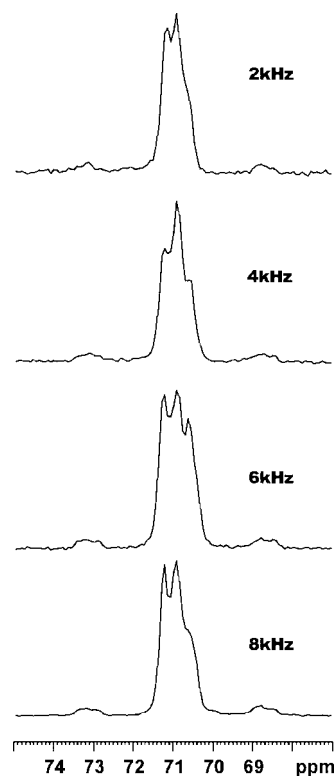


**FIGURE 2.** <sup>31</sup>P CP/MAS spectra of complex **2A** obtained with different MAS frequencies as indicated.

From the analysis of the spectrum, the presence of the three components **1**, **2**, and **3** in the solid state is obvious.

However, before we began to analyze the data, we addressed the crucial question of how representative is the sample under investigation (PS) to the material studied by means of other techniques, e.g., X-ray diffraction of a single crystal (SXRD).

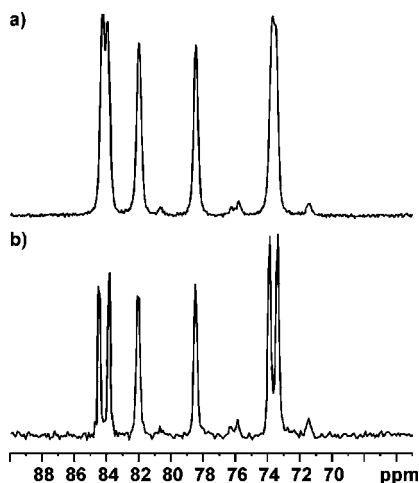


**FIGURE 3.** Experimental  $^{31}\text{P}$  NMR spectra of three component sample crystallized from toluene: (a) powdered sample (PS) recorded with CP/MAS sequence and spinning rate 8 kHz; (b) three-components single crystal (TCSC) A held in rotor filled with silica gel recorded with CP/MAS sequence and spinning rate of 8 kHz. Note the much better NMR resolution of resonance lines and small distinction of  $^{31}\text{P}$  chemical shifts for the monocystal compared to powdered sample.

In our case, at least two options have to be taken into consideration: first, a mixture of single crystals (MSC) when the sample consists of three separated single crystals of each compound before powdering, and second, the three-component single crystal (TCSC), with three isostructural dichalcogenides in the unit cell.

Figure 3b shows the  $^{31}\text{P}$  CP/MAS spectrum of a single crystal held in silica gel and spun in a zirconium rotor at 8 kHz. Much better resolution of signals and small distinction of  $^{31}\text{P}$  chemical shifts for disulfide and diselenide doublets in Figure 3b is apparent. From analysis of the spectra, it is clear that intensity of resonance lines of components in Figure 3a and b is comparable. A  $^{31}\text{P}$ – $^{31}\text{P}$  proton-driven spin diffusion (PDS) 2D experiment<sup>12</sup> (Figure 4) enables us to conclude that we have a crystal composed of compounds **1**, **2**, and **3** (TCSC A) rather than MSC.

The strong dipole–dipole couplings between the  $^{31}\text{P}$  nuclei allows spatial proximities to be directly probed within a distance of 15 Å. The homonuclear dipole–dipole coupling conveys information about the distance of a pair of nuclei and is expressed by the equation  $R_{\text{dip}} = -(\mu_0/8\pi^2)\gamma^2 h/d^3$ , where  $d$  is the internuclear distance and  $\gamma$  is the magnetogyric ratio. The  $R_{\text{dip}}$  value at a  $^{31}\text{P}$ – $^{31}\text{P}$  length of 4.4 Å is 231 Hz, for 13 Å it is 9 Hz, and for 19 Å it is ca. 3 Hz. Beyond these distances, we should not observe cross-peaks in a 2D plot. Employing the 2D PDS experiment with a relatively long mixing time of 10 s establishes remote connectivities between phosphorus sites in the unit cell.

Figure 5 presents  $^{77}\text{Se}$  CP/MAS spectra of PS TCC A recorded with slow sample spinning. Due to the large chemical shift anisotropy, a number of spinning sidebands flanking the isotropic lines are observed. The distinction of  $^{77}\text{Se}$  chemical shifts for isotropic values of component **2** and **3** is equal to  $\Delta\delta = 60$  ppm. The  $\delta_{\text{iso}}$  values are found to be 329.2 ppm for **2** and 389.6 ppm for **3**. The isotropic resonances are labeled by asterisks.

In the next step, we focused our attention on TCC having different guest molecules in the crystal lattice. The NMR spectrum for powdered sample crystallized from propan-2-ol

(PS TCC B) is shown in Supporting Information. Comparing  $^{31}\text{P}$  CP/MAS spectra for PS TCC A and PS TCC B, it is seen that the crystal lattice architecture for both samples is different. In the latter case we have eight  $^{31}\text{P}$  signals in the isotropic part of the spectrum.

**2. Analysis of Thermal Processes in the Solid State and Reversible Guest Molecules Diffusion.** In previously published papers, we have proved that below the melting temperature, disulfide **1** undergoes complex thermal processes related to guest migration from the crystal lattice.<sup>3</sup> Similar phase alternation was observed for diselenide **2**. Differential scanning calorimetry (DSC) was used to establish the temperatures of desolvation and of melting.  $^{31}\text{P}$  CP/MAS NMR confirmed the change of symmetry of molecules above 353 K. After the phase transition, the whole molecule is an asymmetric part of the unit cell. The phosphorus signals P1 and P2 are separated about 3 ppm.

The more intriguing question is the behavior of the mixture of disulfide **1** and diselenide **2** with an increase in temperature, in particular in relation to the solid-state synthesis of **3** described in section 1. A DSC profile of the mixed sample is shown in Figure 6a. Since solid-state NMR is the technique that allows us to understand and explain the macroscopic results on a molecular level, in this project we have employed a complementary approach joining DSC and NMR. Figure 7 shows the variable temperature (VT) CP/MAS study of a gently ground mixture of **1** and **2** in a 1:1 ratio.

The bottom spectrum (333 K) illustrates the mixture of **1** and **2** with clear cut signals of both components. At a temperature of 343 K, the slow rearrangement of disulfide is observed. At a slightly higher temperature, diselenide **2** is changed and a release of toluene is observed. At a temperature which corresponds to a strong exothermic peak on DSC, the new NMR signals appear. We assume that at this temperature a chemical process takes place and compound **3** is synthesized. However, the obtained mixture contains more signals than in the case of PS TCC A.

In order to avoid ambiguities in signals assignment, we have carried out VT NMR measurements of PS TCC A (Figure 7, upper spectrum). A DSC profile is shown in Figure 6b. As in the previous case with an increase in temperature, changes for disulfide **1** and diselenide **2** are observed. In the NMR spectrum, the shifting of  $^{31}\text{P}$  isotropic peaks is apparent. Comparing the upper spectra shown in Figure 7, it can be concluded that in both cases (mixture **1**, **2** and PS TCC A), the final product is very similar. The appearance of two new  $^{31}\text{P}$  signals is noteworthy, as they were not seen in the starting material. Since their assignment is equivocal, we have employed a 2D approach to see all short-range connectivities in the crystal lattice of TCC A before and after heating. For this purpose, we used an experiment which employs a double quantum (DQ) strategy<sup>14</sup> and a POST-C7 sequence which is characterized by a large DQ efficiency and is easy to implement<sup>15</sup> (see Supporting Information).

Finally, it is interesting to note that the process of thermal removal of the guest molecule from the crystal lattice of TCC is reversible and the guest can be introduced back into the matrices by diffusion. The rate of this process can be followed by a  $^{31}\text{P}$  CP/MAS experiment. Figure 8 shows the spectra of sample recorded just after heating (a), after 20 min (b), after 40 min (c) and after 1 h of diffusion (d).

A thermally treated sample was kept in a closed vessel filled with toluene without direct contact between host and guest. As

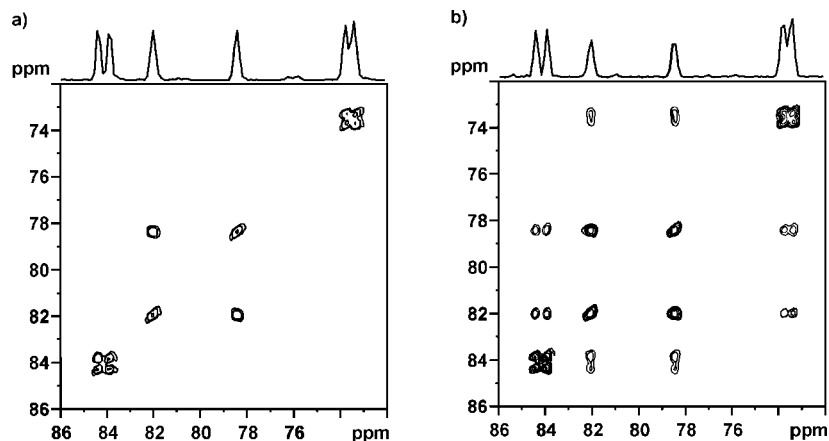


FIGURE 4.  $^{31}\text{P}$ – $^{31}\text{P}$  proton driven spin diffusion 2D correlation recorded with mixing times of (a) 0.2 and (b) 10 s.

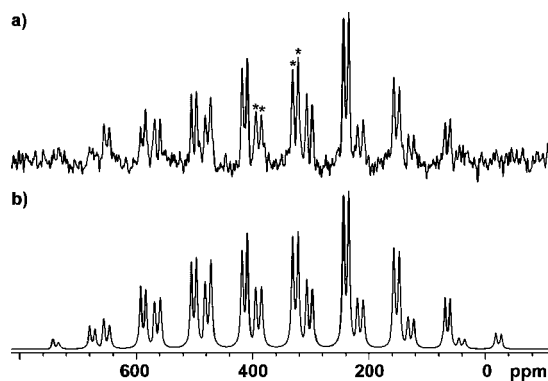


FIGURE 5. Experimental  $^{77}\text{Se}$  CP/MAS NMR spectrum for PS TCC A: (a) recorded with spinning rate 5 kHz, and (b) the best fitted  $^{77}\text{Se}$  spectrum obtained using the SIMPSON program.<sup>13</sup>

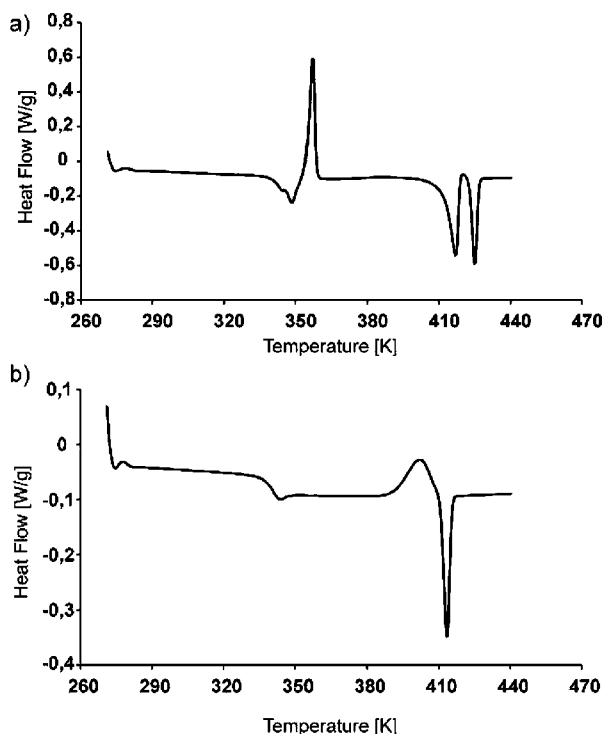


FIGURE 6. (a) DSC profile of mixture of disulfide **1** and diselenide **2** crystallized in toluene. (b) Second run of mixture shown in (a).

one can see after 1 h, this process is completed. From this result, we can conclude that upon guest removal the main skeleton of

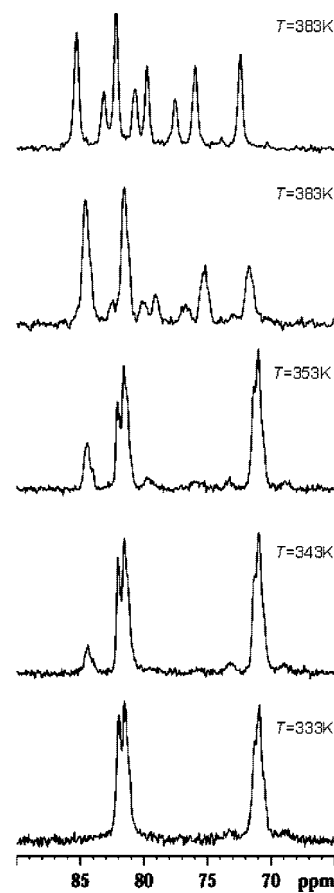
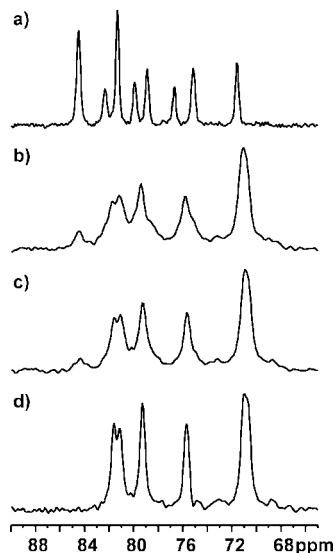


FIGURE 7. Variable temperature (VT)  $^{31}\text{P}$  CP/MAS NMR spectra of mixture **1A** and **2A** with toluene in the crystal lattice recorded with a spinning rate of 8 kHz. The temperatures of measurement are indicated in the right column. The top spectrum represent sample PS TCC A recorded at a temperature of 383 K.

host molecules retained their structure and the stability of the host framework below the melting temperature is pretty high. Similar behavior was observed for diselenide **2**.

After removal of guest, the host framework is rearranged but in the presence of toluene the starting architecture of the crystal is renewed after 40 min. A more complex picture was observed when we exchanged guest molecules, replacing toluene with propan-1-ol. As in the previous case, sample **2** crystallized from toluene after thermal treatment below the melting temperature was kept in a closed vessel filled with propan-1-ol without direct



**FIGURE 8.** Reversible guest exchange in the crystal lattice of **PS TCC A**. The top  $^{31}\text{P}$  CP/MAS NMR spectrum shows sample after thermal treatment at 383 K. Sample was kept at room temperature in the opened 4 mm NMR rotor aligned in a closed vessel filled with toluene. Sample after (a) thermal treatment, (b) 20 min of contact with toluene vapor, (c) 40 min of contact with toluene vapor, and (d) 1 h of contact with toluene vapor.

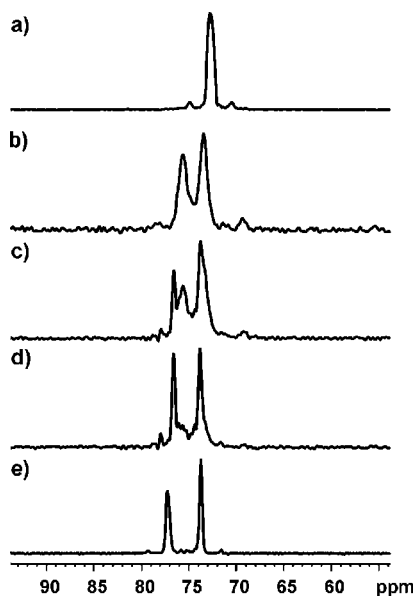


**FIGURE 9.** Reversible guest exchange in the crystal lattice of **2A**. (a) Sample with toluene in the crystal lattice, (b) spectrum after thermal treatment at 383 K. Thermally treated sample was kept at room temperature in the opened 4 mm NMR rotor aligned in a closed vessel filled with propan-1-ol. Sample after (c) 2 h of contact with vapors of propan-1-ol and (d) 12 h of contact with vapor of propan-1-ol. (e) Sample **2** crystallized with propan-1-ol.

contact between host and guest. The process of guest exchange is much slower compared to the reversible migration of toluene and is completed after 24 h.

Figure 9 presents a few stages of guest migration monitored by means of a  $^{31}\text{P}$  CP/MAS technique. It is interesting to note that the final form of host–guest complex (diselenide **2** with propan-1-ol) obtained by diffusion is slightly different compared to crystals obtained from propan-1-ol. In the former complex, the difference between isotropic signals is 2.8 ppm, whereas in the later form  $^{31}\text{P}$   $\Delta\delta_{\text{iso}}$  is equal to 3.5 ppm.

**3. Single-Crystal X-Ray Diffraction Study of Bis[6-*O*,6-*O'*-(1,2:3,4-Diisopropylidene- $\alpha$ -*D*-galactopyranosyl)thiophosphoryl] Dichalcogenides.** Determination of crystal and molecular structures of diselenide **2** with toluene (**2A**), propan-2-ol (**2B**), and propan-1-ol (**2C**) was straightforward. These structures are free from Se/S scrambling phenomena that occurs in the structures of TCSC widely discussed below. The X-ray data for diselenides **2** with toluene, propan-2-ol, and propan-1-ol are included as Supporting Information.

The structure solution and refinement of TCSCs with toluene (**A**), propan-2-ol (**B**) and propan-1-ol (**C**) is more complicated than the refinement of the diselenides **2** because it is impossible to make a distinction between S and Se atoms when Mo  $K\alpha$  radiation is used. According to the Cambridge Structural Database (Version 02.2007) the mean S–S and Se–Se bond lengths in a P=S/Se–S/Se=P system are 2.03 and 2.33 Å, respectively (see Supporting Information).

Thus S and Se atoms are likely to occupy almost identical crystallographic positions in the Se/S–Se/S bridges. A typical refinement procedure applicable in the case of such an atom scrambling is to assign them equal coordinates. Therefore the bond lengths of hypothetical chains Se–Se, S–Se, Se–S, S–S cannot be precisely defined. We could, however, retrieve accurate statistical data of major occupancies of chalcogen sites. Similar phenomena were reported by Aucott et al. for N-(diphenylselenio)diphenyl-sulfimidium tetraphenylborate and for bromide salt.<sup>16</sup> Useful scrambled atom position information (for Se in particular) might be obtained by means of X-ray measurements at wavelengths below and above the selenium absorption edge. Such an experiment might be conducted on a synchrotron beamline and could be the subject of further studies.

**3.1. SXRD study of TCSC A.** This sample crystallizes in the C2 space group with half of the formula unit in the asymmetric unit. Crystallographic data, structure and experimental details are given in Supporting Information.

The S=P–S/Se–S/Se–P=S backbone adopts an *anti-anti* geometry (with S=P–S/Se–S/Se–P=S). Due to the Se/S scrambling, the Se/S–Se/S bond lengths cannot be accurately measured. Consequently the Se/S–P distance cannot be found. On the contrary, the thionophosphoryl (P=S) bond is equal to 1.916 Å, which is within the typical range for bis(organothio-phosphoryl) compounds. The relative occupancy of the disordered Se/S bridge was refined to 60%:40% (which is consistent with NMR observations). The anisotropic displacement parameters of pairs Se1/S1 were constrained to be identical. The full set of geometrical parameters for TCSC **A** are given as Supporting Information.

The host:guest ratio for **A** is 1:2 and interactions between the hosts and toluene are stabilized by a weak hydrogen bond C1A–H24···C4L with a length of 2.88 Å. The C–H···O bonding between host and guest molecules suggests the solvated structure of **A**. The host–host C–H···S=P stabilizing bond of 3.86 Å is visible in a structure solution of **A**. We do not,

(12) Szeverenyi, N. M.; Sullivan, M. J.; Maciel, G. E. *J. Magn. Reson.* **1982**, *47*, 462–475.

(13) Bak, M.; Rasmussen, J. T.; Nielsen, N. C. *J. Magn. Reson.* **2000**, *147*, 296–330.

(14) Dusold, S.; Sebald, A. *Annu. Rep. NMR Spectrosc.* **2000**, *41*, 185–264.

(15) (a) Eden, M.; Levitt, M. H. *Chem. Phys. Lett.* **1998**, *293*, 173–179. (b) Hohwy, M.; Jakobsen, H. J.; Eden, M.; Levitt, M. H.; Nielsen, N. C. *J. Chem. Phys.* **1998**, *108*, 2686–2694.

(16) (a) Aucott, S. M.; Dale, S. H.; Elsegood, M. R. J.; Gilby, L. M.; Holmes, K. E.; Kelly, P. F. *Acta Crystallogr., Sect. C: Cryst. Struct. Commun.* **2005**, *61*, O112–O113.

however, observe this type of interaction ( $C-H\cdots S=P$ ) between host and guest molecules.

**3.2. SXRD Study of TCSC B and TCSC C.** The crystals of both complexes crystallized in the trigonal crystal system in the  $P3_2$  space group. Crystallographic data and experimental details are included as Supporting Information. The structure of the former compound is shown in Supporting Information (Figure 5).

As in the case of **A**, samples **B** and **C** display *anti-anti* geometry of the  $Se/S-Se/S-P=S$  moieties. The resemblance of bond lengths, bond angles, and torsion angles is apparent (see Supporting Information). Positional disorder ( $Se/S$  scrambling) also occurs in the structures of **B** and **C**, and hence the  $Se/S-P$  bond lengths cannot be precisely determined. The  $P1=S1$  and  $P2=S2$  bond lengths are 1.912 and 1.917 Å, respectively, for **B** and 1.918 and 1.917 Å, respectively, for **C**.

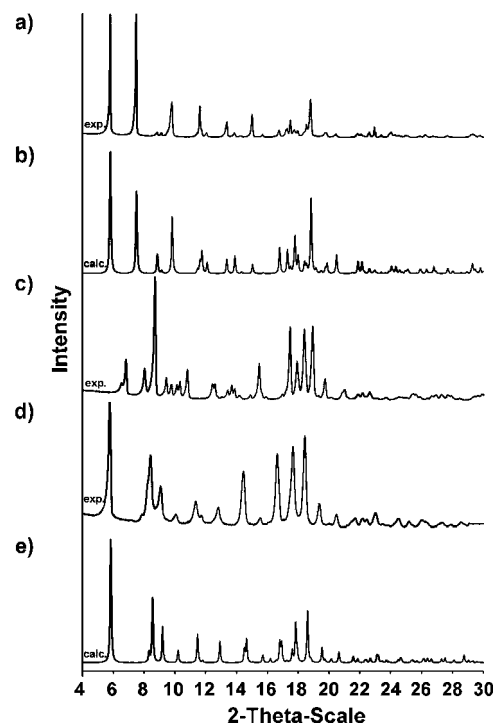
Interestingly the refinement of the site occupancies of the chalcogen atoms in the bridges, conducted by the same method as for **A**, resulted in considerably different values for **B** and **C**. In the structure of **A** the selenium site occupancy was refined to an average value of 61%; however, the same refinement conducted for **C** resulted in a 51% selenium occupancy. This may indicate differences among the compounds present in the crystallization mixture in ability to propagate crystal growth. The anisotropic displacement parameters of the pairs of atoms  $Se1/S1$  and  $Se2/S2$  were constrained to be identical.

Apart from the positional disorder in the  $Se/S$  bridge in the structure of **B**, solvent disorder is also apparent. The major occupancy for the solvent was refined to 41%. The host to guest ratio in structures of **B** and **C** is 1:2, the same as that determined for **A**. In contrast to **A**, molecules of propan-2-ol and propan-1-ol are occluded within the crystal lattice in cage and channel formed by host molecules. The guest molecules in **B** (propan-2-ol) are stabilized in the lattice by hydrogen bonds:  $O1L2-H26\cdots O1L1$ . Similar H-bonds are observed for propan-1-ol in **C**.

The  $C-H\cdots S=P$  bond (3.61 Å in length) is known to significantly contribute to formation of inclusion complexes.<sup>3</sup> The same type of interaction ( $C-H\cdots S=P$ ) is also used to link host molecules and is observed in both the **B** and **C** structures.

For all of the structures described in section 3, the galactopyranose rings bonded to phosphorus adopt a distorted twist conformation, due to the presence of five-membered rings of isopropylidene groups (see CIF files in Supporting Information).

**4. Correlation between Solid-State NMR and XRD.** In the previous section we reported data obtained by means of SXRD and SS NMR for single crystals and powdered samples. Significant recent progress has been made in diffraction method for powdered solids (XRDP).<sup>17</sup> Powder diffraction pattern contain essentially the same information as pattern for single crystal. In the later case the diffraction data are distributed in three-dimensional space, whereas the diffraction data of powders are “compressed” into one dimension pattern. As a consequence, there is usually considerable overlap of peaks in the powder diffraction diagram. Despite appearing sometimes interpretation problems the XRDP is technique of choice for investigation of mechanism of phase transition, molecular distortion, polymorphism, etc. when the selection of single crystals or crystal with proper quality is difficult or impossible. Moreover, XRDP provides the bridge between SXRD and SS NMR of powdered samples.



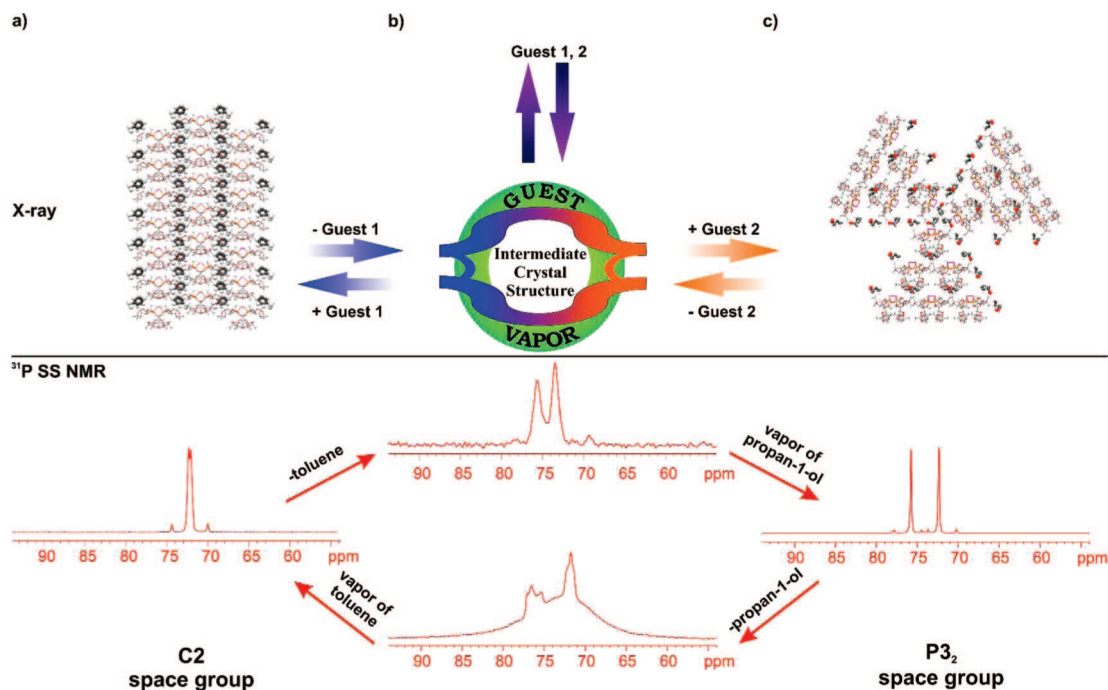
**FIGURE 10.** Experimental and calculated powder X-ray diffraction patterns of the three crystallographic forms of **2**: (a) experimental pattern of sample crystallized in toluene, **2A**; (b) calculated pattern of **2A**; (c) experimental pattern of **2A** after guest removal (intermediate crystal structure, ICS); (d) experimental XRD pattern of ICS sample kept a few hours in contact with propan-1-ol vapors; (e) calculated pattern of **2** crystallized in propan-1-ol, **2C**.

Figure 10a shows the XRDP pattern for diselenide **2** with toluene occluded in the crystal lattice (**2A**), and Figure 10c is the sample after thermal guest removal below the melting temperature (intermediate crystal structure, ICS). Experiments discussed here exactly follow the NMR observations shown in Figure 9.

In the next step the sample was closed in the vessel filled with propan-1-ol vapors and kept a few hours. XRDP data for such treated sample is displayed in Figure 10d. Figure 10b and e show the calculated powder patterns for **2A** ( $C2$  space group) and **2C** ( $P3_2$  space group), respectively. In both cases SXRD data were taken as input files.

In the host–guest assembly (space group  $C2$  of host), molecular columns of host diselenides and TCSC host–guest complexes form supramolecular structures with columnar architecture. In the complex of diselenide **2** with toluene, molecular columns of the host are in parallel orientation along all the crystallographic axes, whereas in the structures of diselenide **2** with propan-2-ol and propan-1-ol (space group  $P3_2$ ) the orientation is along the screw 3-fold axis. Our XRD and SS NMR study clearly prove that for systems under investigation we observe reversible crystallographic space group change stimulated by exchange of guest. The process of changes of crystal lattice parameters is shown in pictorial form in Figure 11. Supramolecular arrays presented in Figure 11a ( $C2$  space group) and Figure 11c ( $P3_2$  space group) were constructed employing SXRD coordinates. ICS is characterized by SS NMR and XRDP.

It is worthy to note that in the exchange process beginning from the complex including propanol-1-ol in the host matrix (**2C**) in contact with vapor of toluene we obtained sample **2A**.



**FIGURE 11.** Schematic pathway of reversible space group change: (a) supramolecular array of complex of diselenide **2** with toluene, **2A**; (b) ICM crystals surrounded by vapor of guest molecules; (c) supramolecular array of complex diselenide **2** with propan-1-ol. The bottom traces below the solid line show appropriate  $^{31}\text{P}$  CP/MAS spectra for crystalline complexes and intermediate crystal structures.

In this case, the structure of the intermediate product is slightly different. The full pathway of reversible space group exchange investigated by means of  $^{31}\text{P}$  NMR spectroscopy is shown at the bottom in Figure 11. We observed a similar behavior of samples when single-crystals of **2A** and **2C** were investigated.

It is also worthy to note that in the exchange process beginning from the complex including *n*-propanol in the host matrix in contact with toluene vapor we obtained sample **2A**. However, the structure of the intermediate product is slightly different. The full cycle pathway of reversible space group exchange investigated by means of  $^{31}\text{P}$  NMR spectroscopy is included as Supporting Information.

A problem that is worth highlighting in regard to solid-state studies of TCSC crystals is related to molecular disorder. Two kinds of molecular disorder can be distinguished, dynamic related with molecular motion in the crystal lattice and static. Subtle structural features, e.g., deviation from perfect periodicity (static distortion), have influence on the physical properties of condensed matter. This subject was recently exhaustively reviewed by Ravy et al.<sup>18</sup> Sehnert and Senker have reported a concerted approach for determination of the local environment in ordered and disordered phases in the solid state.<sup>19</sup> The case of TCSC seems to be very special. XRD and SSNMR spectroscopy do not answer the question regarding the organization of components 1, 2, and 3 in the unit cell. It is also not clear whether such periodicity exists or if the arrangement of components is random (e.g., 1, 2, 3; 2, 1, 3; etc.). In the case of these structures the chalcogen atoms scrambling phenomena is observed. Therefore the bond lengths and corresponding angles of hypothetical chains cannot be precisely defined. We can however retrieve the accurate statistical data of major occupan-

cies sites. Moreover, the guest migration disturbs the structure of the host making a disordered lattice. The crucial host–guest interactions can be easily attained from the structure solution of TCSC.

## Conclusions

In this work we have employed a complementary approach to determine crystal and molecular structure of inclusion complexes, the rate and mechanism of reversible guest exchange, and the molecular disorder of the lattice. Traditionally, the structural aspects of crystal samples have been limited to results obtained by means of diffraction techniques. Harris has recently reported that NMR crystallography can be employed for determination of crystallographic asymmetric units, of molecular symmetry in the solid-state environment, and crystallographic space group assignment.<sup>20</sup> Furthermore, Taulelle has shown that solid-state NMR spectroscopy offers suitable tools for space group determination.<sup>21</sup> In this project, we showed that analysis of  $^{31}\text{P}$  CP/MAS spectra can help in the proper choice of the space group. The  $^{31}\text{P}$  *J*-coupling experiment and dependence of line shape versus rotor spinning rate, characteristic for samples that have symmetry 2 (sample **2A**) and the fact that this effect is not observed for complexes with  $3_2$  symmetry (samples **2B** and **2C**) further support the above discussed approach.

In this work, we also report the first example of the formation of selenenyl sulfide linkages in the solid phase. Determining the driving force of this process is a crucial and intriguing question. It is well-known that a diselenide bond is weaker than a disulfide bond by nearly 20 kcal/mol. Bachrach et al. have recently reported results of computational studies of the mechanism of nucleophilic attack at selenium in diselenides and

(17) Harris, K. D. M.; Cheung, E. Y. *Chem. Soc. Rev.* **2004**, *33*, 526–538.

(18) Ravy, S.; Launois, P.; Moret, R.; Pouget, J.-P. *Z. Kristallogr.* **2005**, *220*, 1059–1065.

(19) Sehnert, J.; Senker, J. *Chem. Eur. J.* **2007**, *13*, 6339–6350.

(20) Harris, R. K. *Solid State Sci.* **2004**, *6*, 1025–1037.

(21) Taulelle, F. *Solid State Sci.* **2004**, *6*, 1053–1057.



selenenyl sulfides in both the liquid and gas phases.<sup>22</sup> It was concluded that selenium is more polarizable than sulfur, making it a better nucleophile and a better leaving group. Our efforts to isolate the selenenyl sulfide **3** from a reaction mixture failed since **3** can exist only in an equilibrium mixture with **2** and **1** both in the liquid and solid phases. As we showed, NMR spectroscopy is a convenient tool which allows us to follow the progress of a reaction in the solid state and to establish the yield of products.

Finally, we wish to draw attention to the diagnostic features of SS NMR for investigating the rate and mechanism of reversible guest exchange in the crystal lattice of the host. Pluth and Raymond recently exhaustively discussed the problem of the guest exchange mechanism in supramolecular host–guest assemblies.<sup>23</sup> The power of liquid-state NMR spectroscopy and such techniques as NOESY, ROESY, DOSY, etc. was clearly demonstrated. On the other hand, knowledge about applications of NMR spectroscopy in the solid state is not very common. In this project, we showed that host matrices, and crystallographic space groups are changed during the reversible guest exchange and this process can be easily followed by a <sup>31</sup>P CP/MAS experiment.

## Experimental Section

A scheme showing synthetic pathway **A** and **B** is included as Supporting Information.

**Synthesis of Compounds 1, 2, and 3.** Chlorodithiophospholane (i) (0.72 g, 4.6 mmol) and triethylamine (0.64 mL, 4.6 mmol) were added dropwise to a solution of 1,2:3,4-diisopropylidene- $\alpha$ -D-galactopyranose (ii) (1.0 g, 3.8 mmol) in CH<sub>2</sub>Cl<sub>2</sub> (50 mL). The reaction was carried out under nitrogen conditions, and the mixture was stirred at room temperature until the hydrogen chloride evolution ceased. After ca. 0.5 h, S<sub>8</sub> (0.15 g, 4.6 mmol, path **A**) or Se (0.73 g, 9.2 mmol, path **B**) was added, and the stirring was continued for 1 or 24 h, respectively. Water (50 mL) was then poured into the mixtures, and the reaction products were extracted with CH<sub>2</sub>Cl<sub>2</sub> (3  $\times$  20 mL). The extracts were dried over anhydrous magnesium sulfate and concentrated under reduced pressure. The residue was either purified by short column chromatography (eluent CH<sub>2</sub>Cl<sub>2</sub>) in path **A** or used for the next step without purification in path **B**.

In the following reaction stage, products obtained [iii, 1.48 g, 3.6 mmol (path **A**) or 1.72 g, 3.7 mmol (path **B**)] were dissolved in 30 mL of CH<sub>2</sub>Cl<sub>2</sub> and the next portion of 1,2:3,4-diisopropylidene- $\alpha$ -D-galactopyranose (**A**, 0.94 g, 3.6 mmol; **B**, 0.96 g, 3.7 mmol in 10 mL of CH<sub>2</sub>Cl<sub>2</sub>) and triethylamine (0.6 mL, 4.3 mmol) were added into both solutions. After reaction at room temperature for ca. 24 h and the addition of water (40 mL), products were removed from mixtures by extraction with CH<sub>2</sub>Cl<sub>2</sub> (3  $\times$  20 mL). The organic layers were isolated, dried (MgSO<sub>4</sub>), and concentrated under vacuum to give iv (**A** and **B**).

Depending on the desired product, the triethylamine 6-*O*,6'-*O*-(1,2:3,4-diisopropylidene- $\alpha$ -D-galactopyranosyl)dithiophosphoric acid salt (iv, **A**) or 6-*O*,6'-*O*-(1,2:3,4-diisopropylidene- $\alpha$ -D-galactopyranosyl)selenothiothiophosphoric acid salt (iv, **B**) or the same equivalents of both iv (**A**) and i (**B**) salts were oxidized with iodine in a toluene–water system until the iodine color disappeared. Unreacted iodine was utilized by a saturated aqueous solution of sodium sulfite. The toluene extracts were isolated and dried over anhydrous magnesium sulfate. The excess of solvent was removed under vacuum and the product was crystallized from toluene. According to this procedure,

the following compounds were prepared: bis[6-*O*,6'-*O*-(1,2:3,4-diisopropylidene- $\alpha$ -D-galactopyranosyl)dithiophosphoryl] disulfide (**1**); bis[6-*O*,6'-*O*-(1,2:3,4-diisopropylidene- $\alpha$ -D-galactopyranosyl)dithiophosphoryl] diselenide (**2**); and bis[6-*O*,6'-*O*-(1,2:3,4-diisopropylidene- $\alpha$ -D-galactopyranosyl)dithiophosphoryl] selenyl-sulfide (**3**).

All described conversions were monitored by <sup>31</sup>P NMR spectroscopy.

**NMR Measurements.** The solid-state CP/MAS experiments were performed on the spectrometer at 75.47 MHz frequency for <sup>13</sup>C, equipped with a MAS probe head using 4-mm ZrO<sub>2</sub> rotors. A sample of glycine was used for setting the Hartmann–Hahn condition and adamantane was used as a secondary chemical shift reference  $\delta = 38.48$  and 29.46 ppm from external TMS.<sup>24</sup> The conventional spectra were recorded with a proton 90° pulse length of 3.5  $\mu$ s and a contact time of 1 ms. The repetition delay was 10 s and the spectral width was 25 kHz. The FIDs were accumulated with a time domain size of 2000 data points. The RAMP shape pulse<sup>25</sup> was used during the cross-polarization and TPPM decoupling<sup>26</sup> with  $\tau_p = 6.8 \mu$ s and a phase angle of 20° during the acquisition. The cross-polarization efficiency was measured with contact times between 10  $\mu$ s and 12 ms. The spectral data were processed using the WIN-NMR program.<sup>27</sup> Simulations of the spinning CSA sidebands spectra were carried out on a PC using the SIMPSON program on the Linux operating system.

<sup>77</sup>Se 57.203 MHz spectra were recorded on the spectrometer at 300.00 MHz frequency for <sup>1</sup>H, equipped with MAS probe head using 4-mm ZrO<sub>2</sub> rotors. Diammonium selenate was employed to set up the Hartmann–Hahn condition. The 90° pulse was 4.0  $\mu$ s, the contact time 4 ms, the spectral width 50 kHz, and the time domain 4 kHz. One thousand scans were accumulated for each experiment. The <sup>77</sup>Se chemical shifts were calibrated indirectly through ammonium selenate used as a secondary chemical shift reference standard, set at  $\delta = 1040.2$  ppm (using dimethyl selenide as the primary reference,  $\delta = 0$  ppm). For <sup>31</sup>P NMR, 85% phosphoric acid was employed as a primary standard. The conventional spectra were recorded with a proton 90° pulse length of 3.5  $\mu$ s and a contact time of 1 ms. The repetition delay was 10 s and the spectral width was 25 kHz. POST-C7 experiments were carried out with an MAS frequency of 10 kHz. The appropriate r.f. pulse nutation frequency was 70 kHz. 2D spectra were recorded with the  $t_1$  increment synchronized with the rotor period; 48  $t_1$  serial files were collected for each experiment. The 2D spectra were processed with Qsine apodization functions equal to 2.5 in both dimensions.

**X-Ray Analysis.** Block-shaped crystals of **2A**, **2B**, **2C**, **TCSC B**, and **TCSC C**, and a prism-shaped crystal of **TCSC A** were used for the X-ray measurements. The crystals of inclusion complexes were obtained at ambient temperature by slow isothermal crystallization of host molecules dissolved in appropriate solvents. The diffraction data were collected at 103 K using diffractometer, equipped with a Mo K $\alpha$  radiation source and Mo radiation at room temperature ( $\omega$  scan). The structures were solved by the HKL-3000SM system.<sup>28–30</sup>

The X-ray powder diffraction patterns were measured in a reflection mode on powder diffraction system equipped with a Bragg–Brentano PW 3050/65 high resolution goniometer and PW 3011/20 proportional point detector. The Cu K $\alpha$ 1 radiation was

(22) Bachrach, S. M.; Demoin, D. W.; Luk, M.; Miller, J. V. *J. Phys. Chem. A* **2004**, *108*, 4040–4046.

(23) Pluth, M. D.; Raymond, K. N. *Chem. Soc. Rev.* **2007**, *36*, 161–171, and references therein.

(24) Morcombe, C. R.; Zilm, K. W. *J. Magn. Reson.* **2003**, *162*, 479–486.  
(25) Metz, G.; Wu, X.; Smith, S. O. *J. Magn. Reson. Ser. A* **1994**, *110*, 219–227.

(26) Bennett, A. W.; Rienstra, C. M.; Auger, M.; Lakshmi, K. V.; Griffin, R. G. *J. Chem. Phys.* **1995**, *103*, 6951–6958.

(27) *Win-NMR*, Version 6.0; Bruker-Franzen Analytik GmbH: Bremen, Germany, 1993.

(28) Otwinowski, Z.; Borek, D.; Majewski, W.; Minor, W. *Acta Crystallogr. A* **2003**, *59*, 228–234.

(29) Minor, W.; Cymborowski, M.; Otwinowski, Z.; Chruszcz, M. *Acta Crystallogr. D* **2006**, *62*, 859–866.

(30) Sheldrick, G. M. *SHELXS97* and *SHELXL97*; University of Gottingen: Germany, 1997.

used. The patterns were measured at 291.0(2) K in the range 2–90° with the narrowest beam attenuator.

**Acknowledgment.** The authors would like to thank Professor Maria Gdaniec for helpful discussion and comments.

**Supporting Information Available:** Scheme of synthesis,  $^{31}\text{P}$ – $^{31}\text{P}$  2D POST C7 NMR spectra of **TCSC A** before and

after thermal phase transition,  $^{31}\text{P}$  CP/MAS spectra of **TCSC B**, histogram with S–S and Se–Se bond length distribution. CIF files of complexes **2A**, **2B**, **2C** and **TCSC A**, **TCSC B**, **TCSC C**. This material is available free of charge via the Internet at <http://pubs.acs.org>.

JO8002997